

LFT Modeling and μ Analysis of the Aircraft Landing Benchmark

Andrea Iannelli* Pedro Simplício* Diego Navarro-Tapia*
Andrés Marcos*

* *University of Bristol, BS8 1TR, United Kingdom (Technology for
AeroSpace Control (TASC), www.tasc-group.com; e-mail:
andrea.iannelli/pedro.simplicio/diego.navarro-tapia/andres.marcos@bristol.ac.uk)*

Abstract: The landing of a civil transport aircraft is one of the most challenging phases. The reason mainly lies in the need to satisfy different concurrent requirements in the face of a wide range of system variations and environmental perturbations. Automatic control laws have been developed in the past to address this complex scenario, using an involved iterative process of design, tuning and validation. Due to the uncertainties and perturbations present in this phase, robust synthesis techniques (e.g. standard and structured \mathcal{H}_∞ design) provide an effective framework to accomplish these tasks. This compels on the other hand to rely on procedures to generate the proper mathematical description of the plant and the availability of analysis tools to obtain time efficient robust predictions and insight into the system being analyzed. This work presents the application of Linear Fractional Transformation modeling and μ analysis to the Aircraft Landing Benchmark proposed by ONERA and Airbus.

Keywords: LFT modeling, robust performance, sensitivity analysis, aircraft landing challenge

1. INTRODUCTION

The final approach and flare of a civil transport aircraft are critical phases due to the high number of variables to be controlled simultaneously and the high safety standards demanded. Automatic landing control laws have been proposed and put in practice in order to overcome potentially critical landing conditions. However, it is acknowledged (Sadat-Hoseini et al. (2013)) that the process leading to the definition of feedback control laws to successfully accomplish these phases is far from being a consolidated and reliable methodology.

On the one side, due to the concurrent objectives to be achieved, a multi-objective optimization process is required which makes the tuning phase arduous despite the availability of complete design frameworks (Looye and Joos (2006)). On the other side, the automatic landing control has to be proven robust to a wide range of uncertainties belonging to the system (e.g. mass, CG position) and environment (e.g. wind speed, temperature).

Addressing these shortcomings, ONERA and Airbus proposed an Aircraft Landing Challenge (Biannic and Boda-Bauxell (2016)), whose goal is to design an autoland control system to perform approach and landing satisfying a set of certification requirements defined at touch-down. The validation campaign to certify the proposed design is performed in a Monte Carlo (MC) framework employing the provided nonlinear simulator to quantify mean and risk dispersion in the face of the assigned variability in the flight conditions.

This paper focuses on the application of robust modeling and analysis techniques and show that they are instru-

mental tools that provide invaluable insight for the control design stage in this complex scenario. The LFT models and robust μ analyses performed complemented and guided the designs for the benchmark developed by the TASC group (see for example Navarro-Tapia et al. (2017) for the flare component design). The proposed strategy is essential in providing the mathematical models required by the synthesis algorithms in order to achieve the defined robust objectives. In the analysis part of this paper, it is illustrated how the tools provide reliable indications on the performance of the systems within a time frame and manner compatible with the design stage.

The techniques employed in this work are Linear Fractional Transformation (LFT) modeling and structured singular value- μ analysis (Zhou et al. (1996); Packard and Doyle (1993)). These tools are well-established in the research community and have been adopted in the last decades to cope with diverse problems in the control field. Since the system under investigation is defined by means of a realistic nonlinear model aircraft landing, the first step consists in recasting the plant into the LFT framework through a three-step procedure detailed in Sec. 2. Different LFTs are presented therein, along with possible motivations for these choices. In Sec. 3 the capability of μ in evaluating robust performance properties of the systems is detailed, with particular attention to the comparison between the baseline controllers provided with the benchmark and the TASC design proposed for the challenge. In Sec. 4 it is discussed how the capabilities of μ can be further exploited in order to examine more in depth the system and understand possible effects of control design choices. Sec. 5 presents the main conclusions of the work.

2. LFT MODELING OF THE AIRCRAFT LANDING

This Section describes the procedure adopted in order to build LFT models of the aircraft landing system, starting from the provided nonlinear model. A cursory description of the LFT framework follows. Refer to Zhou et al. (1996) for a comprehensive discussion on the topic.

2.1 LFT background

Let \mathbf{M} be a complex matrix termed *coefficient matrix* and partitioned as

$$[\mathbf{M}] = \begin{bmatrix} \mathbf{M}_{11} & \mathbf{M}_{12} \\ \mathbf{M}_{21} & \mathbf{M}_{22} \end{bmatrix} \quad (1)$$

\mathcal{F}_u , namely the upper LFT, is the closed-loop transfer matrix from input \mathbf{u} to output \mathbf{y} when the nominal plant, represented by \mathbf{M}_{22} , is subject to a perturbation matrix $\Delta_{\mathbf{u}}$ (Fig. 1). \mathbf{M}_{11} , \mathbf{M}_{12} and \mathbf{M}_{21} reflect a priori knowledge on how the perturbation affects the nominal map. Once all varying or uncertain parameters are *pulled out* of the nominal plant, the problem appears as a nominal system subject to an artificial feedback. The algebraic expression for \mathcal{F}_u is given by:

$$\mathcal{F}_u(\mathbf{M}, \Delta_{\mathbf{u}}) = \mathbf{M}_{22} + \mathbf{M}_{21} \Delta_{\mathbf{u}} (\mathbf{I} - \mathbf{M}_{11} \Delta_{\mathbf{u}})^{-1} \mathbf{M}_{12} \quad (2)$$

This LFT is well posed if and only if the inverse of the term $(\mathbf{I} - \mathbf{M}_{11} \Delta_{\mathbf{u}})$ exists.

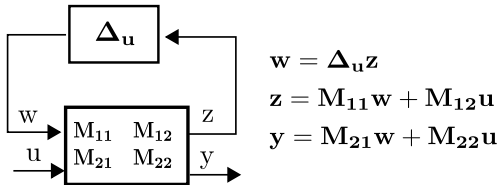


Fig. 1. Upper LFT

2.2 Building LFT models

The LFT modeling paradigm pivots on the algebraic manipulation of linear plants in order to recast the problem as depicted in Fig. 1. In the present application, the system is described by means of a Simulink nonlinear model of a civil transport aircraft (Biannic and Boada-Bauxell (2016)). The routine *ACStrim* is provided in order to perform longitudinal trim and linearization once a particular flight condition is specified through the input argument *flightpar*. This aircraft benchmark challenge consists in designing a controller to enable landing despite parametric variations. This means that some of the parameters specifying the flight condition are described by a range of values. As a result, each possible flight condition generates a Linear Time-Invariant (LTI) system. A three-step procedure is developed in order to obtain a representative LFT.

Firstly, the set of parameters ρ affecting the linearization (i.e. belonging to the *flightpar* argument) is selected. In this work two sets are considered: the first holds Mass (m), Center of Gravity longitudinal position (x_{CG}), Runway altitude (h_{rwy}) and Temperature (T_0), whereas the second includes also the Longitudinal Wind speed (WX). This choice is made in order to study the effects on design and analyses of considering two distinct LFTs differing in size and in the ability to capture a parameter believed

a priori to be relevant for the challenge (i.e. WX). Once an appropriate number of samples of these variables has been chosen, the routine *ACStrim* is employed to evaluate the linearized LTI systems (A_i, B_i, C_i, D_i) associated to the i^{th} combination of the samples.

Secondly, a linear plant ($\mathbf{A}(\rho), \mathbf{B}(\rho), \mathbf{C}(\rho), \mathbf{D}(\rho)$) with a polynomial or rational dependence on the uncertain parameters is generated. This task is accomplished by means of the APRICOT library (Roos et al. (2014)) of the SMAC toolbox. In particular in this work the routine *olsapprox* is adopted, which performs orthogonal least-square in order to obtain a polynomial approximation for a set of samples obtained for different values of some explanatory variables. The main output is an object defining for each entry of the polynomial, parameter-dependent LTI matrix the coefficients and exponents of the monomials employed in the approximation. After several tests, the maximum degree of the approximating polynomial has been fixed to 1.

The final step consists in converting the system into an LFT. An embedded capability of the APRICOT library enables to directly generate the LFT as output of the *olsapprox* routine. However, the approximation obtained at the previous step is further manually manipulated in order to reduce the size of the final LFT. The parameter dependence of some entries are removed based on physical assumptions (e.g. neglected dependence on ρ of some coupling terms between longitudinal and lateral dynamics) and numerical assessment. For the latter, the magnitude of the polynomial coefficients are compared to that for the nominal value, and those below a defined tolerance discarded. The manually *reduced* symbolic object is finally transformed into the desired LFT by means of the GSS library (Biannic and Roos (2016)), which employs sophisticated realization techniques to accomplish this task.

The accuracy of the LFT is a prerequisite for an effective application of this framework. When the LFT is employed to reproduce a nonlinear system, it is recommended to perform both linear and nonlinear validations (Marcos et al. (2006)). A representative set of flight conditions inside the allowed range of variation of the parameters is defined. For the linear validation, this set is used to generate the corresponding LTI systems (by means of *ACStrim*) which are compared in terms of Bode magnitude and eigenvalues with those obtained through realization of the LFT specifying the corresponding values of Δ . For the nonlinear validation, the family of LTI systems given by the LFT and corresponding to the selected set of samples is time-simulated and a comparison with analogous nonlinear simulations (in terms of response around the trim points) is attempted, in terms of time-variation of meaningful variables. This twofold strategy has been employed for all the LFT models discussed in the sequel, obtaining satisfactory results as later shown.

2.3 Different LFT options

The LFTs generated by means of the outlined procedure serve two main purposes. On the one side, they are employed for the synthesis of feedback control laws with linear robust techniques (Navarro-Tapia et al. (2017)). On the other, it is an essential framework for the application of the μ -based robust analyses. For these reasons, different LFTs

are built and employed in the study. A first distinction, in terms of the set of parameters included in the Δ block, has been already mentioned in Sec.2.2. A second important one concerns the LTI system adopted for the polynomial interpolation in the second step discussed before. A first obvious choice is to consider the dynamics directly derived from the linearization routine. They consist of 16 states, 9 inputs and 19 measured outputs. After examining the involved variables, the LTI for the study of the full dynamics of the aircraft can be reduced to 13 states, 7 inputs and 9 outputs listed below (refer to Biannic and Boada-Bauxell (2016) for the notation):

$$\begin{aligned} \mathbf{x}_{\text{FULL}}^{13} &= u, v, w, p, q, r, \phi, \theta, \psi, \delta_T, \delta_A, \delta_E, \delta_R \\ \mathbf{u}_{\text{FULL}}^7 &= \delta_{T_c}, \delta_{A_c}, \delta_{E_c}, \delta_{R_c}, w_x, w_y, w_z \\ \mathbf{y}_{\text{FULL}}^9 &= n_y, n_z, p, q, r, \phi, v_c, v_z, \chi \end{aligned} \quad (3)$$

where the size of the vector is recalled in the superscripts.

In order to tailor the design of the controllers to specific performance objectives, and in view of the physical decoupling between motions, it is of interest to study separately the reduced dynamics for the longitudinal and lateral plane. In particular, this leads respectively to:

$$\begin{cases} \mathbf{x}_{\text{LON}}^6 = u, w, q, \theta, \delta_T, \delta_E \\ \mathbf{u}_{\text{LON}}^4 = \delta_{T_c}, \delta_{E_c}, w_x, w_z; & \mathbf{y}_{\text{LON}}^4 = n_z, q, v_c, v_z \\ \mathbf{x}_{\text{LAT}}^7 = v, p, r, \phi, \psi, \delta_A, \delta_R \\ \mathbf{u}_{\text{LAT}}^3 = \delta_{A_c}, \delta_{R_c}, w_y; & \mathbf{y}_{\text{LAT}}^5 = n_y, p, r, \phi, \chi \end{cases} \quad (4)$$

Tab.1 gives the size for the different derived LFT models:

LFT	without WX	with WX
Longitudinal	24	29
Lateral	19	26
Full	39	51

Table 1. LFTs size

In Fig.2 it is depicted an example of nonlinear validation applied to the Full LFT (set without WX) with the uncertainties fixed at their maximum values. In order to perturb the trim a step-input in longitudinal and lateral wind disturbances (i.e. w_y and w_z) is considered and the two responses are observed in terms of load factors n_y and n_z , longitudinal velocity V_c and roll angle ϕ . Note that the LFT is able to capture adequately the transient, although some features (in particular with reference to n_y and n_z , e.g. different overshoots and non-minimum phase behaviour) are missed.

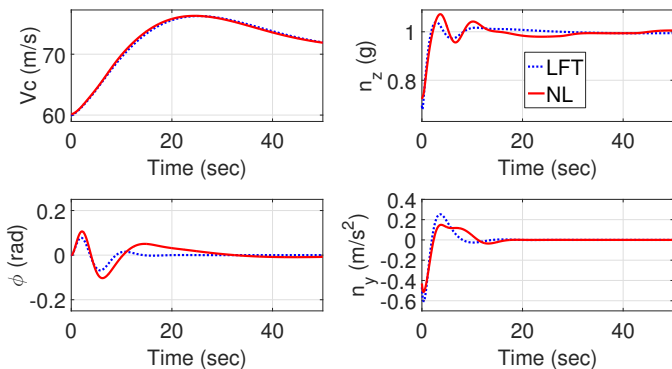


Fig. 2. Nonlinear time-domain validation of the full LFT

3. ROBUST ANALYSIS OF THE CHALLENGE

This Section describes the robust analyses performed on the derived LFT models. The analyses presented in this work consider two controllers: the baseline provided with the benchmark (Biannic and Boada-Bauxell (2016)) and the one designed by the TASC team for the challenge.

Traditionally, an autopilot landing can be split in three phases: the final approach, flare and decrab. In the first, considered here, the ILS vertical (glide-slope) and lateral (localiser) errors must be minimised while keeping the calibrated airspeed V_c constant and the sideslip angle β close to zero. The final approach controllers K_{LON} and K_{LAT} were separately designed using the structured \mathcal{H}_∞ optimisation framework (Gahinet and Apkarian (2011)). K_{LON} is a third-order controller with little coupling between δ_{T_c} and δ_{E_c} , which relies on the measurement of \mathbf{y}_{LON} . In addition, K_{LAT} is a second-order system with pure integration of n_y and ϕ errors, which takes \mathbf{y}_{LAT} as feedback vector.

Following a brief description of the theory underpinning μ analysis (Packard and Doyle (1993)), results are presented and discussed. Unless otherwise indicated, the LFTs without wind are employed.

3.1 μ background

The structured singular value (s.s.v.) is a matrix function denoted by $\mu_\Delta(M)$ and defined as:

$$\mu_\Delta(M) = \frac{1}{\min_{\Delta}(\bar{\sigma}(\Delta) : \det(I - M\Delta) = 0)} \quad (5)$$

where $\bar{\sigma}(\Delta)$ is the maximum singular value of Δ . This definition can be specialized to determine whether the LFT $\mathcal{F}_u(\mathbf{M}, \Delta_u)$ defined in Eq.2 is well posed once the generic matrix M in the above definition is replaced by \mathbf{M}_{11} and Δ belongs to the corresponding uncertainty set Δ_u . For ease of calculation and interpretation, Δ is typically norm-bounded $\|\Delta\|_\infty < 1$ (without loss of generality by scaling of M). In this manner, if $\mu_\Delta(M) \leq 1$ then the result guarantees that the analyzed system represented by the LFT is robustly stable (RS) to the considered uncertainty level. The s.s.v. can be used also for robust performance (RP), which is the application mostly sought here.

Performance here consists in checking whether a closed loop transfer matrix $T(s)$, in terms of its $\|\cdot\|_\infty$ norm, satisfies a frequency domain template $\Psi(\omega)$:

$$\bar{\sigma}(T(j\omega)) < \Psi(\omega) \quad (6)$$

In order to address this task within μ analysis, the idea is to consider two perturbation matrices: Δ_1 is taken as the structured model perturbation Δ_u early introduced and originated by the uncertainties affecting the plant. Δ_2 is instead a full-complex perturbation matrix closing the lower loop in Fig. 1 by connecting the signals \mathbf{y} and \mathbf{u} . This *fictitious* block, which doesn't reflect any actual perturbation of the plant, is introduced to take advantage of the Main Loop Theorem (Zhou et al. (1996)). This theorem ensures that the condition $\mu_\Delta(\mathbf{M}) < 1$ is a test for the robust performance of the plant represented by the LFT. It's worth noticing that \mathbf{M} is now employed and not \mathbf{M}_{11} as for the RS test.

It is known that μ calculation is non-polynomial (NP)

hard, thus the algorithms implement upper and lower bound calculations (Balas et al. (2005)).

3.2 Analysis of Longitudinal dynamics

The LFT employed in this section is obtained closing the longitudinal plant defined in Eq.4 with the baseline controller and K_{LON} . The LFT employed is defined by the uncertain block Δ_{LON} :

$$\Delta_{LON}^{24,R} = \text{diag}(\delta_m I_6, \delta_{x_{CG}} I_6, \delta_{h_{rwy}} I_6, \delta_{T0} I_6) \quad (7)$$

where the size of the uncertainties and their nature (R stands for real) is recalled in the superscripts. In Fig. 3 the RS of the two controllers is investigated. The predicted values of μ are well below 1 for the whole frequency range. This ensures large RS for both systems, expected since performance is the main concern in this problem. For this reason, in the rest of the article the focus is to RP.

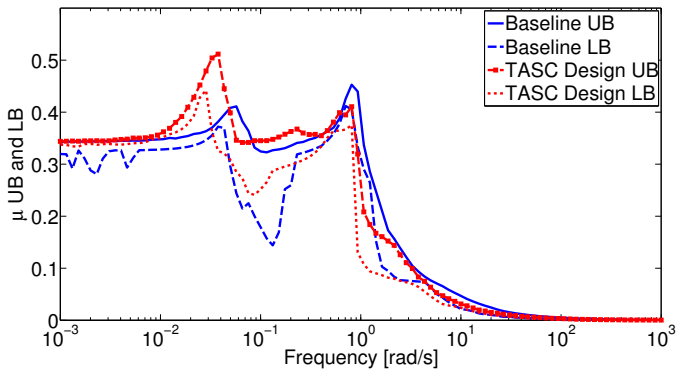


Fig. 3. Longitudinal Plant RS with two controllers

In Fig. 4 robust performance is considered. For each closed loop, the μ UB (LB is very close to it) and the maximum singular values (MSV), which are a measure of the nominal performance, are shown. The results show that both the nominal and robust performance improve for the TASC design. Note that this improvement is with respect to the specific weights used for the TASC design, and thus the results for the baseline design must be taken with care. Nonetheless, this improvement was confirmed with a nonlinear simulation campaign.

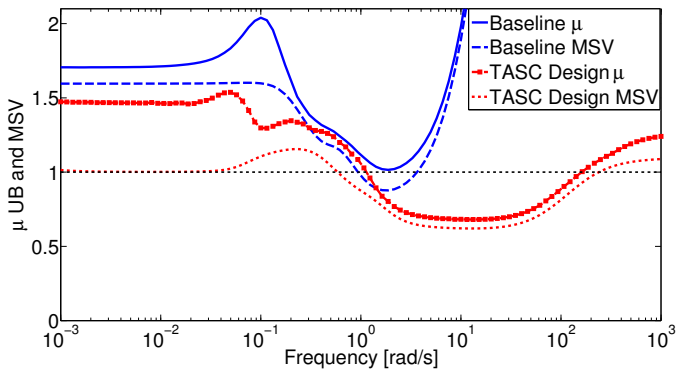


Fig. 4. Longitudinal Plant RP with two controllers

3.3 Analysis of Lateral dynamics

Robust performance is here evaluated for the lateral plants, closed with the lateral baseline controller and

K_{LAT} , employing the LFT defined by the uncertain block Δ_{LAT} :

$$\Delta_{LAT}^{19,R} = \text{diag}(\delta_m I_6, \delta_{x_{CG}} I_5, \delta_{h_{rwy}} I_4, \delta_{T0} I_4) \quad (8)$$

Fig. 5 shows the lateral RP comparison. It is worth noting that the TASC design ensures a value of μ UB equal or smaller than 1 in all the frequency range and a substantial improvement in the high frequency range.

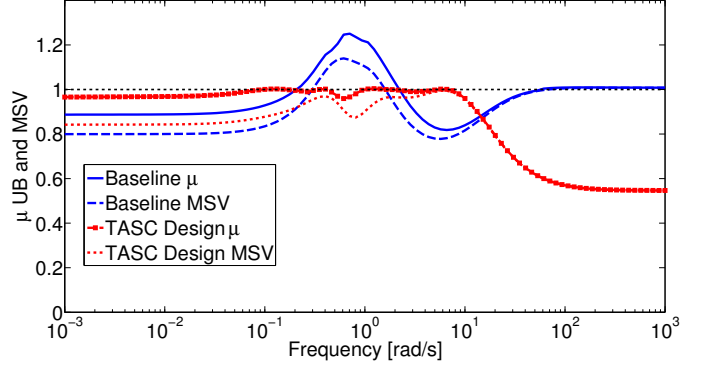


Fig. 5. Lateral Plant RP with two different controllers

An interpretation of the result in Fig. 5 is that the baseline closed-loop (featuring a peak $\mu_M^B \simeq 1.25$) can only guarantee a degradation of RP of a factor 1.25 for an uncertainty range of 80% ($\simeq \frac{1}{1.25}$) the current analyzed one. The TASC design on the other hand guarantees the fulfillment of the requirements within the defined range of uncertainties (as it is $\mu_M^T < 1$). In order to confirm these considerations, a robust performance assessment via nonlinear simulations evaluated at scattered flight conditions (i.e. using 100 random runs) is performed. Three cases are considered: baseline and TASC closed-loops with the full uncertainty range (respectively K_{Base} and K_{LAT}), and baseline with the above 80% range ($K_{Base-\mu}$). Fig. 6 shows the Gaussian fits of the distributions at touch-down for 4 parameters: lateral deviation from runway Y_{LG} , lateral load factor n_y , roll rate p and yaw rate r . The dispersion in the values with respect to the nominal value (null for all of them) is a measure of loss in performance of the system. The plot hence confirms the predictions of Fig. 5: K_{LAT} features always a better behaviour than K_{Base} ; $K_{Base-\mu}$ has comparable performance to K_{LAT} . In that respect, it is worth remarking that the employed parameters are not directly connected to the frequency-domain performance requirements analysed by μ and thus they are here proposed only as *indicators* of loss of robustness. See (Marcos et al. (2015)) for a thorough discussion on this approach taken to reconcile μ predictions with nonlinear simulation.

3.4 Analysis of the Full system

For control design purposes, the system has been considered decoupled and thus longitudinal and lateral dynamics treated separately. This section addresses the analysis of the full plant (Eq.3) closed with the full TASC autoland control design. The aim is to provide a general assessment on the performance behavior of the full closed-loop system in the face of the considered uncertainties, as well as to check the validity of the aforementioned *decoupled* design approach. The defined uncertain block Δ_{FULL} is given by:

$$\Delta_{FULL}^{39,R} = \text{diag}(\delta_m I_{11}, \delta_{x_{CG}} I_{10}, \delta_{h_{rwy}} I_9, \delta_{T0} I_9) \quad (9)$$

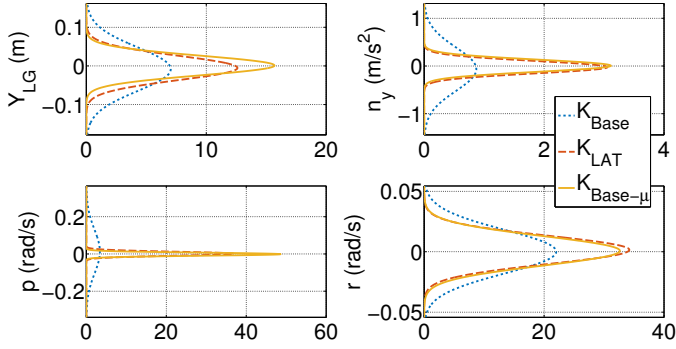


Fig. 6. Result of MC runs for lateral variables

Fig. 7 shows the RP upper μ bound comparison for the longitudinal, lateral and full closed-loops, with the TASC controllers. It is apparent that the full μ envelops the corresponding values obtained for the decoupled plants. The relatively negligible importance of the coupling terms could have been inferred looking at the Bode plot of the full nominal plant. However, the information shown here is more general since it ensures that these terms do not play a decisive role even when uncertainties are involved, which is more difficult to state a priori.

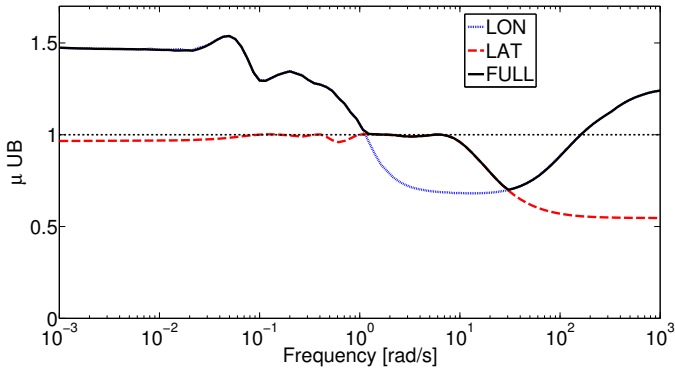


Fig. 7. RP analysis of the TASC controllers with long, lat and full LFTs

3.5 Effect of Longitudinal Wind as uncertainty

Next, the effect of the longitudinal wind (captured as an uncertain parameter) is investigated. In Fig. 8 it is shown, for each reduced dynamics, the degradation in terms of RP when WX is included. The longitudinal plant seems barely affected by the addition of this uncertainty, whereas the lateral plant is sensitive in the low frequency range, showing for the rest an unchanged trend. This aspect can be connected with the violation of one limit risk requirement for the TASC design in extreme wind conditions.

4. SENSITIVITY ANALYSIS AND INSIGHTS

Sec.3 has shown how μ analysis can be employed in order to predict degradation of nominal performance of a closed loop plant in the face of uncertainties defined by a LFT. Another application of this tool consists in performing a sensitivity analysis of either RS or RP with respect to the set of uncertainties. Once a condition is defined (determinant condition in Eq.5 for RS, violation of the frequency template in Eq.6 for RP), μ highlights the relevance of the generic term in Δ in determining it.

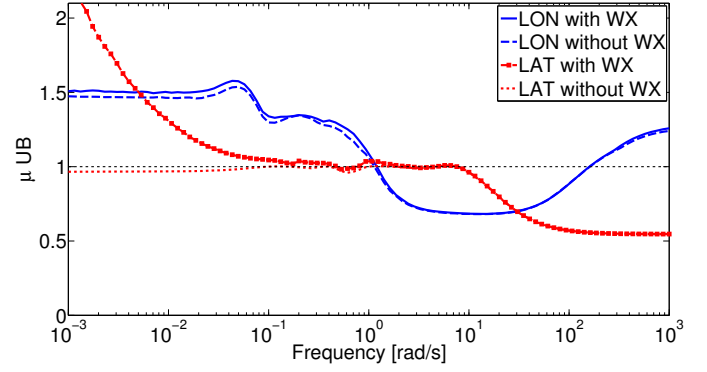


Fig. 8. Effect of adding WX in the LFT (TASC design only)

Although more advanced μ sensitivity analyses can be employed using the skew- μ concept (Ferrerres and Biannic (2003); Marcos et al. (2005)), in here the sensitivity estimate implemented in the Robust Control Toolbox (Balas et al. (2005)) is used. It employs a finite difference calculation where the uncertainty range of the considered uncertainty is enlarged (default value 25%) and the percentage loss in robust margin is evaluated.

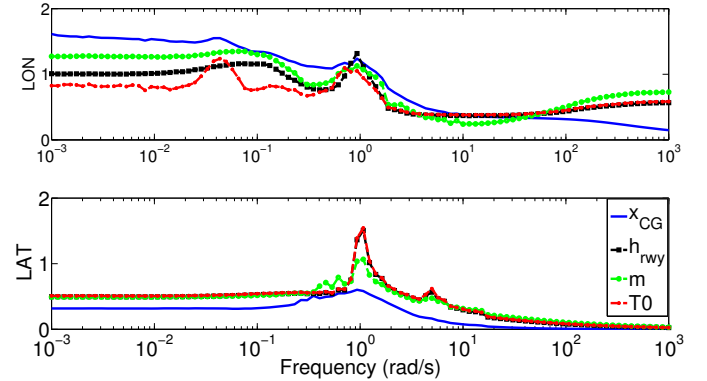


Fig. 9. Sensitivity of RP to the uncertain parameters for Longitudinal and Lateral plant

The results for the plants controlled with the TASC design are shown in Fig. 9. Different trends can be detected: the longitudinal plant is mostly affected by x_{CG} and m , whereas the lateral shows similar sensitivity to all the parameters except CG which is the less critical. This last information is in accordance with physical understanding. Sensitivity analysis can also be applied to the input channels \mathbf{u} of the LFT. This option is not directly available within the Toolbox, but the analysis can be approached as follows. As known, a scaling of the submatrices \mathbf{M}_i (defining \mathbf{M} in Eq.1) is equivalent to shrink/enlarge the size of the associated blocks in Δ . Once the LFT modeling step is performed, and thus the coefficient matrix \mathbf{M} is available, the sub-partition related to the considered input into the plant can be identified and weighted.

This procedure is applied here to study the effect on RP of two inputs: reference signals and wind disturbance (i.e. w_x , w_y and w_z). These analyses can provide further insight on the RP behaviour of the closed loop and thus prompts a rationale to improve the controller design. In Fig. 10 a comparison between the sensitivity of the lateral baseline and TASC designs is provided. The corresponding plot for the longitudinal plant shows similar features.

Two expected trends are detectable in the plots. The sensitivity to reference input is greater at low frequencies and drops as this is increased, whereas the opposite happens for the wind. An interesting feature emerges when the sensitivity to wind disturbances is compared between baseline and TASC designs. These have a similar trend until approximately $10 \frac{rad}{s}$, after which the wind sensitivity is considerably reduced for the second (see the range highlighted by the arrow). It is worth noticing that in the same frequency range Fig. 5 showcased a considerable improvement in robustness. In this range of frequencies it can also be observed a greater sensitivity to reference for the TASC design, but this takes place in a region where this input is not believed to be determinant in terms of performance degradation.

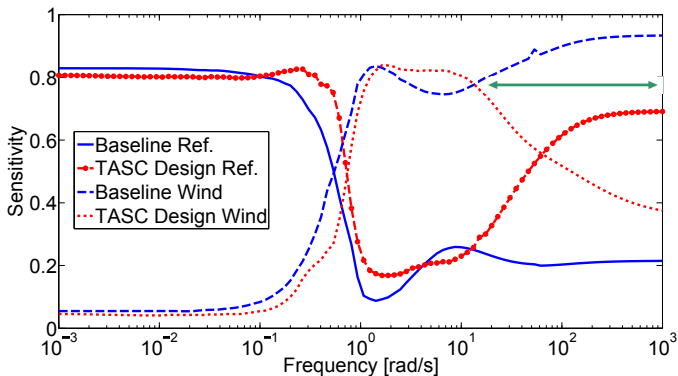


Fig. 10. Sensitivity of RP to the Inputs of the Lateral plant: comparison with baseline

These aspects reflect one of the rationale that guided the design of the robust control laws for both the plants. Preliminary analyses performed by means of MC-based nonlinear simulations seemed to suggest that wind disturbances at the input of the system played prominent role in degrading the requirements of the challenge. The design was then oriented towards a mitigation of this effect. The analysis in Fig. 10 proves this attempt and its achievement within a linear robust framework (such as the one represented by LFT and μ). The complement of these analyses showing the behavior of the designed controllers in terms of the benchmark requirements will be further discussed in future works, and is also partly presented in (Navarro-Tapia et al. (2017)).

5. CONCLUSION

This paper illustrates the application of Linear Fractional Transformation modeling and μ analysis to the Aircraft Landing Benchmark. The overall task of the challenge is to design an autoland control system to satisfy a set of requirements at touch-down in the face of system variations and environment perturbations. This work focuses on the development of LFT models for the synthesis of robust control laws and analysing the closed loop plants so-obtained in terms of robust performance.

The predictions that can be obtained with μ are something more than a simple binomial-type of output (either the system is robust or not within the prescribed uncertainty set). It was shown for example that the sensitivity of the degradation in performance of the system to a single parameter was efficiently captured by μ analysis. Moreover,

this can be applied also to a set of inputs of the plant to detect which ones are more critical in degrading the performance of the plant.

This work shows the potentiality of the framework LFT- μ to cope with this practical challenge. The controllers designed employing the plant models detailed in this work decisively improved the robustness of the system. This accomplishment was certified by means of a Monte-Carlo statistical analysis based on nonlinear simulations.

ACKNOWLEDGEMENTS

The authors wish to thank the ONERA SMAC team for providing the version of the APRICOT (Roos et al. (2014)) routine *olsapprox* without limitations.

REFERENCES

- Balas, G., Chiang, R., Packard, A., and Safonov, M. (2005). *Robust Control toolbox*.
- Biannic, J.M. and Boada-Bauxell, J. (2016). *A Civilian Aircraft Landing Challenge*. On-line available from the aerospace benchmark section of the SMAC Toolbox, <http://w3.onera.fr/smac/>, Toulouse 2016.
- Biannic, J.M. and Roos, C. (2016). Generalized state space: a new matlab class to model uncertain and nonlinear systems as linear fractional representations. Technical report.
- Ferreres, G. and Biannic, J. (2003). Skew Mu Toolbox (SMT): a presentation. Technical report, DCSD, ONERA.
- Gahinet, P. and Apkarian, P. (2011). Structured \mathcal{H}_∞ Synthesis in MATLAB. In *The 18th IFAC World Congress*. Milan, Italy.
- Looye, G. and Joos, H. (2006). Design of autoland controller functions with multiobjective optimization. *Journal of Guidance, Control, and Dynamics*, Vol. 29(2).
- Marcos, A., Bates, D., and Postlewhite, I. (2005). Control oriented uncertainty modeling using μ sensitivities and skewed μ analysis tool. CDC-ECC.
- Marcos, A., Biannic, J., Jeanneau, M., Bates, D., and Postlewhite, I. (2006). Aircraft modeling for nonlinear and robust control design and analysis. 5th IFAC Symposium on Robust Control Design, Toulouse, France.
- Marcos, A., Rosa, P., Roux, C., Bartolini, M., and Benani, S. (2015). An overview of the rfcv project v&v framework: optimization-based and linear tools for worst-case search. *CEAS Space Journal*, 7(2), 303–318.
- Navarro-Tapia, D., Simplício, P., Iannelli, A., and Marcos, A. (2017). Robust Flare Control Design using Structured \mathcal{H}_∞ Synthesis: a Civilian Aircraft Landing Challenge. In *The 20th IFAC World Congress*.
- Packard, A. and Doyle, J. (1993). The complex structured singular value. *Automatica*, 29(1), pp. 71–109.
- Roos, C., Hardier, G., and Biannic, J.M. (2014). Polynomial and rational approximation with the APRICOT library of the SMAC toolbox. Proceedings of the IEEE Multiconference on Systems and Control.
- Sadat-Hoseini, H., Fazlzadeh, A., Rasti, A., and Marzocca, P. (2013). Final approach and flare control of a flexible aircraft in crosswind landings. *Journal of Guidance, Control, and Dynamics*, Vol. 36(4).
- Zhou, K., Doyle, J.C., and Glover, K. (1996). *Robust and Optimal Control*. Prentice-Hall, Inc., Upper Saddle River, NJ, USA.